The Journal of Prevention of Alzheimer's Disease 12 (2025) 100131

Contents lists available at ScienceDirect

The Journal of Prevention of Alzheimer's Disease

journal homepage: www.elsevier.com/locate/tjpad

Original Article

Fingolimod ameliorates amyloid deposition and neurodegeneration in APP/PS1 mouse model of Alzheimer's disease

Meng-Ting Wang[a,1], Zi-Cheng Hu[b,1], Yang Xiang[c,1], Xiao-Qin Zeng[a], Zhang-Cheng Fei[a], Jia Chen[a], Xin-Peng Li[a], Yu-Peng Zhu[a], Jun Wang[a], Yan-Jiang Wang[a,d], Zhi-Qiang Xu[a,*], Yu-Hui Liu[a,d,*]

[a] Department of Neurology and Centre for Clinical Neuroscience, Daping Hospital, Third Military Medical University, Chongqing, PR China
[b] Department of Neurology, The First Affiliated Hospital of Chongqing Medical University, Chongqing, PR China
[c] Institute of Neurology, Sichuan Provincial People's Hospital, School of Medicine, University of Electronic Science and Technology of China, Chengdu, PR China
[d] Key Laboratory of Aging and Brain Disease, Chongqing, PR China

ARTICLE INFO

Keywords:
Alzheimer
Amyloid-beta
Neurodegeneration
Lymphocyte
Fingolimod

ABSTRACT

Introduction: The immune system plays a critical role in regulating amyloid-beta (Aβ) metabolism in Alzheimer's Disease (AD). Both T and B lymphocytes are involved in the pathogenesis of AD. The sphingosine-1-phosphate (S1P) receptor modulator fingolimod used in the treatment of multiple sclerosis, can promote lymphocyte homing, potentially reducing the infiltration of peripheral lymphocytes into the brain.

Methods: In this study, 8-month-old APP/PS1 mice were orally administered fingolimod at a dose of 1 mg/kg/day or saline as a control for 2 months. After treatment, the mice were subjected to behavioral tests, pathological examinations, and biochemical analyses to evaluate behavioral deficits and AD-type pathologies.

Results: Fingolimod inhibits the infiltration of peripheral lymphocytes into the brain and reduces neuroinflammation. Fingolimod enhances cognitive function and alleviates brain Aβ deposition. Additionally, fingolimod treatment mitigates other AD-related pathologies, including Tau hyperphosphorylation, neuroinflammation, and neurodegeneration. Proteomic analysis further confirms the therapeutic effects of fingolimod in AD, reflected by the downregulation of proteins involved in multiple AD-associated pathways.

Discussion: This study illustrates that fingolimod effectively ameliorates multiple pathological features of AD, highlighting its potential as a promising therapeutic candidate for the disease.

1. Background

Alzheimer's disease (AD) is the most common neurodegenerative disorder characterized by progressive memory loss and cognitive decline. Approximately 48 million people worldwide suffer from AD, and the number is expected to triple by 2050 [1]. The accumulation of Amyloid-beta (Aβ) and subsequent formation of intracellular neurofibrillary tangles composed of hyperphosphorylated Tau protein are the major pathological hallmarks and therapeutic targets of AD [2–4]. However, the mechanisms underlying the dysregulation of Aβ metabolism have not been fully elucidated.

The immune system plays a critical role in regulating Aβ metabolism and the development of AD [5–9]. The accumulation of peripheral immune cells in the brain parenchyma can be observed during aging and in AD, potentially contributing to the heightened inflammation in the brain [10]. It is found that longitudinal increase in B lymphocytes is associated with decreased Aβ clearance and increased Aβ deposition in AD patients [11]. Consistently, systemic depletion of B cells is demonstrated to reserve Aβ deposition and other AD-type pathologies in an animal model of AD [12]. Previous studies have also discovered that some subsets of T cells promote Aβ accumulation and neurodegeneration [13,14].

Identifying therapeutic agents from existing clinical drugs holds significant potential, particularly given the lengthy timeline and risks associated with new drug development [15]. Fingolimod is a first-in-class oral sphingosine 1-phosphate receptor (S1PR) modulator, which is approved for the treatment of relapsing-remitting multiple sclerosis [16]. It impacts the trafficking of T and B cells, as well as oligodendrocytes, where S1PR5 receptors are expressed. Additionally, fingolimod prevents the disruption of the blood-brain barrier, which may inhibit the infiltra-

* Corresponding authors at: Department of Neurology and Centre for Clinical Neuroscience, Daping Hospital, Third Military Medical University, Chongqing, PR China.
E-mail addresses: xzq881@163.com (Z.-Q. Xu), yuhuiliu@tmmu.edu.cn (Y.-H. Liu).
[1] Authors contributed equally to this work.

https://doi.org/10.1016/j.tjpad.2025.100131
Received 14 January 2025; Received in revised form 1 March 2025; Accepted 10 March 2025
2274-5807/© 2025 The Author(s). Published by Elsevier Masson SAS on behalf of SERDI Publisher. This is an open access article under the CC BY-NC-ND license (http://creativecommons.org/licenses/by-nc-nd/4.0/)

tion of peripheral insults into the brain [17,18]. Therefore, considering the autoimmune aspects of AD pathogenesis and the mechanisms of action of fingolimod, we propose that it could be a promising candidate for the treatment of AD.

2. Materials and methods

2.1. Animals

The APPswe/PSEN1dE9 transgenic (APP/PS1) mice used in this experiment were obtained from the Jackson Laboratory (Bar Harbor, ME, USA). This transgenic AD mouse model carries the human amyloid precursor protein (APP) gene, along with the Swedish mutation of the human presenilin 1 (PS1) gene [19]. To eliminate the potential influence of gender differences on AD pathology, only female mice were used in this study. The mice were housed in a controlled environment with a temperature of 22 ± 2°C, a humidity of 45 %±10 %, and a 12-hour light/dark cycle. All experimental procedures were approved by the Experimental Animal Welfare and Ethics Committee of Daping Hospital, Third Military Medical University.

2.2. Treatment

Twenty 8-month-old APP/PS1 mice (n=20) were randomly divided into the treatment group and the control group. Mice in the treatment group were orally treated with fingolimod in the drinking water at a dose of 1 mg/kg/day for 2 months according to previous studies [20,21]. Mice in the control group were treated with saline. At 10 months of age, the animals were euthanized with an overdose of pentobarbital (0.08 g/kg) and perfused with filtered phosphate-buffered saline (PBS) through the heart. One hemisphere of the brain used for histological analyses was fixed in 4 % paraformaldehyde for 24 h, and then placed in a dehydration solution (30 % sucrose in 4 % paraformaldehyde) for 72 h. Subsequently, the brain was embedded in OCT compound, and the hemisphere was cut into 30-μm thick coronal sections across the entire brain using a cryostat. The other hemisphere of the brain was ground into powder with liquid nitrogen. The powder was suspended in RIPA buffer to extract proteins for biochemical analyses.

2.3. Behavioral test

APP/PS1 mice underwent a series of behavioral tests, including the Morris water maze, Y-maze, and open-field test. The Y-maze test consisted of two components: spontaneous alternation and novel arm exploration. The maze consists of three arms arranged at 120° angles. The novel arm exploration test was split into two phases, separated by a 1-hour interval. During the first phase, which lasted 5 min, the mice were allowed to explore two of the arms. In the second phase, the previously blocked arm (the novel arm) was opened, and the mice were placed in the starting arm and given 5 min to explore freely. The number of entries into the novel arm and the time spent there were recorded. To prevent scent cues from influencing behavior, the arms were cleaned with a 75 % ethanol solution between experiments.

In the spontaneous alternation test, each mouse was placed at the end of one arm, facing the wall, and allowed to explore all three arms for 5 min. The alternation percentage was calculated using the following formula: $\text{Alternation percentage} = \frac{\text{Total alternations}}{\text{Total arm entries} - 2} \times 100$. In the open field test, mice were placed in the center of the apparatus and allowed to explore freely for 5 min. Spontaneous activity was measured by recording the total distance traveled. The Morris water maze test was conducted with three platform trials per day. All mice first underwent a pretest to exclude any with impaired swimming ability, which could affect their behavioral performance. During the pretest, mice were allowed to swim for 60 seconds and were then guided to a submerged platform for 1–2 seconds. Afterward, learning trials were conducted over five days, with each mouse performing three 1-minute trials per day, starting from different quadrants. A submerged escape platform was placed in a designated quadrant, and the time it took for each mouse to find the platform was recorded as the escape latency. If a mouse failed to locate the platform, it was guided to it and allowed to stay on it for 5 seconds to familiarize with the location. On the final day of the test, the platform was removed, and several measures were recorded to evaluate the memory of the mice regarding the location of the platform. These included the percentage of time spent in the target quadrant, the swimming trace, and the number of annulus crossing. Video data were analyzed using the ANY-maze software, which measured travelling distance and escape latency during the platform trials. On the sixth day, without the platform, the time spent in each quadrant and at the previous platform location was also recorded.

2.4. Brain sampling and processing

The day after completing the behavioral tests, all mice were euthanized for biochemical and histological analyses. After anesthesia with an intraperitoneal injection of 0.7 % pentobarbital sodium, each mouse underwent intracardial perfusion using 0.1 % $NaNO_2$ in 0.9 % saline. One hemisphere was dissected and fixed in 4 % paraformaldehyde, while the other hemisphere was snap-frozen, ground into powder with liquid nitrogen, and stored at –80 °C. The frozen brain tissue was homogenized in liquid nitrogen, with extracellular proteins extracted using tris-buffered saline (TBS) solution, followed by intracellular protein extraction with RIPA solution, based on a previously established method for future analyses [22].

2.5. Flow cytometry

After treatment, brain samples of mice were processed and homogenized into a paste using Roswell Park Memorial Institute (RPMI) medium (Gibco Thermo Fisher Scientific, USA). The homogenate was then filtered and separated using a Percoll gradient (Cytiva, USA). Following centrifugation at 500 g with minimal braking for 30 min, a distinct white ring was observed at the interface between the 30 % and 70 % layers. Using a pipette, 2–3 ml of the ring-like substance was carefully aspirated into a tube containing 5 ml of PBS. The sample was centrifuged at 500 g for 5 min, and the resulting pellet was resuspended in FACS buffer (Gibco Thermo Fisher Scientific, USA) to a final volume of 100 μl.

To block Fc sites and prevent non-specific fluorescence signals, purified anti-mouse CD16/CD32 antibody (BD Pharmingen, USA) was added at a dilution of 1:100, and the mixture was incubated on ice for 10 min. Following this, anti-mouse PE-CD45R/B220 flow antibody (BD Pharmingen, USA) or anti-mouse FITC-CD3ε (BD Pharmingen, USA) was added and incubated on ice for an additional 30 min. The cells were then washed with cell staining buffer (GibcoThermo Fisher Scientific, USA), resuspended to 100 μl, filtered, and analyzed using a flow cytometer.

2.6. Biochemical analyses

Western blot was employed to analyze the levels of proteins involved in Aβ metabolism, Tau phosphorylation, synaptic plasticity, and neuronal apoptosis. Brain tissue was homogenized in lysis buffer (Invent Biotechnologies, USA) containing phosphatase and protease inhibitors (Roche, CH) using ultrasonic treatment (15 seconds at 20 % pulse), and then incubated on ice for 20 min. The homogenate was centrifuged at 12,000 g at 4 °C for 10 min, and the supernatant was collected and aliquoted for storage at –80 °C. The total protein concentration was determined using a BCA protein assay kit (Beyotime, CHN).

Brain sample proteins were loaded onto an SDS-PAGE gel for electrophoresis. The separated proteins were then transferred onto a nitrocellulose membrane. The blot was probed with a variety of antibodies, including: anti-Aβ (6E10, Biolegend, USA), anti-APP C-terminus (171610, Abcam, UK), which recognizes both full-length APP (APPfl) and C-terminal fragments (CTF)-β; anti-β-secretase (BACE1)

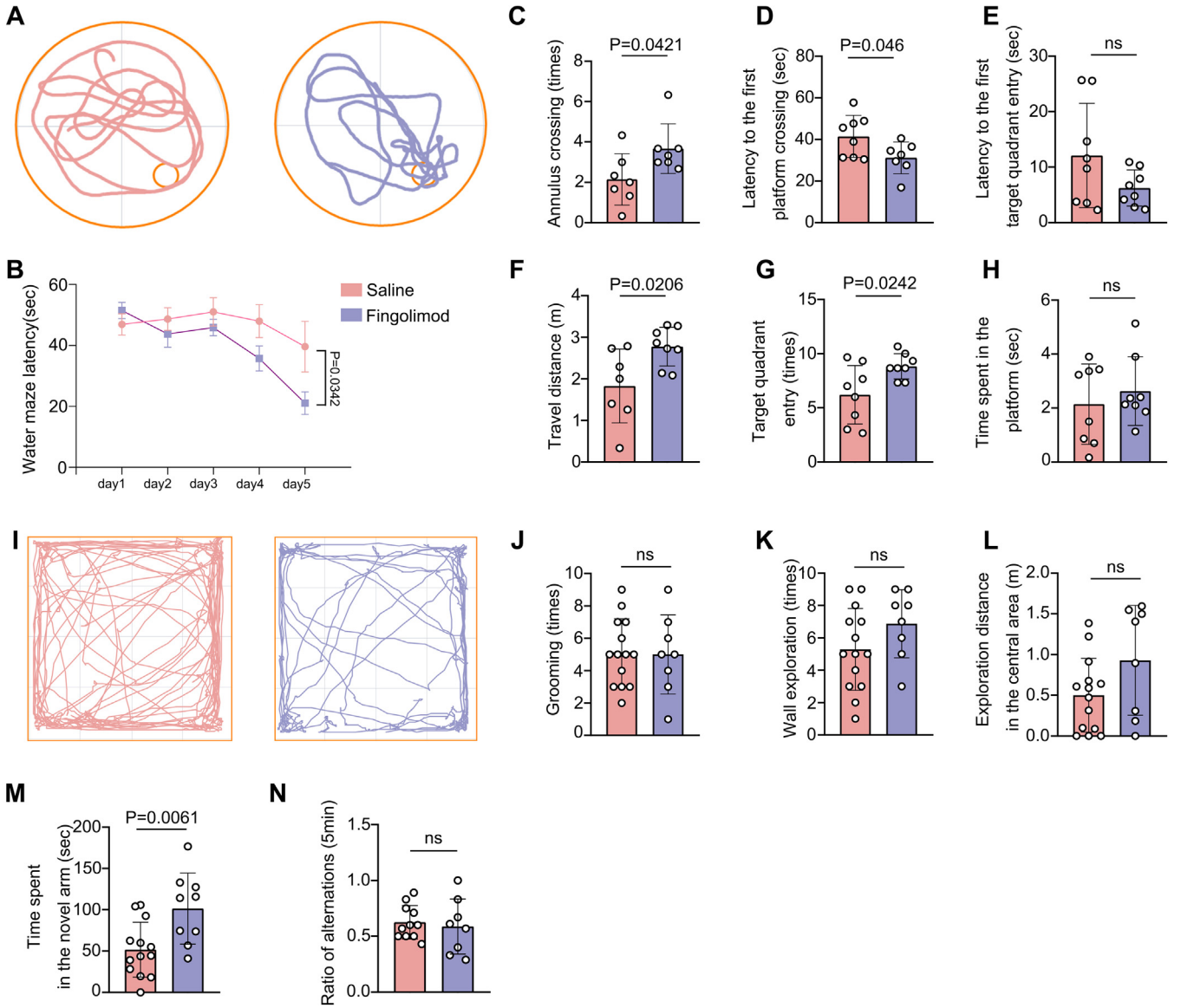

Fig. 1. Fingolimod improves behavioral deficits in APP/PS1 mice. A. Representative tracing graph in the Morris water maze test. B. Escape latency during platform trials in Morris water maze test. C. Number of annulus crossing in probe test. D. Latency to first entry to the target platform in Morris water maze test. E. Latency to first entry to the target quadrant in Morris water maze test. F. Total distance traveled in Morris water maze test. G. Times of target quadrant entry in Morris water maze test. H. Time spent in the platform in Morris water maze test. I. Representative tracing graph in the open filed test. J. Grooming behavior of mice in the open field test. K. Times of wall exploration behavior of mice in the open field test. L.Exploration distance in the central area in the open field test. M.Time spent in the novel arm in the Y-maze test. N. Percentage of alternation novel arm entry in Y-maze test.

(Abcam, UK); anti-presenilin protein 1 (PSEN1) (Cell Signaling, USA); anti-disintegrin and metalloproteinase 10 (ADAM10) (MilliporeSigma, USA); anti-neprilysin (NEP) (MilliporeSigma, USA); anti-advanced glycation end product (RAGE) (Abcam, UK); anti-low-density lipoprotein receptor-related protein (LRP) (MilliporeSigma, USA); anti-insulin-degrading enzyme (IDE) (MilliporeSigma, USA); anti-pS396 (Signalway, USA); anti-pS199 (MilliporeSigma, USA); anti-pT181 (Signalway, USA); anti-pT231 (Signalway, USA); anti-pS404 (Signalway, USA); anti-Tau5 (Signalway, USA); anti-VAMP (Abcam, UK); anti-SNAP25 (Abcam, UK); anti-synaptophysin (SYN) (Abcam, UK); anti-PSD95 (Abcam, UK); anti-PSD93 (Abcam, UK); anti-CD19 (Abcam, UK); and anti-β-actin (Cell Signaling, USA). The membrane was subsequently incubated with IRDye 800CW secondary antibodies (LICOR, USA) and scanned using an Odyssey fluorescence scanner. Band density was normalized to β-actin for subsequent analysis. The levels of Aβ40 and Aβ42 (Thermo Fisher Scientific, USA), and TNF-α and IL-1β (Invitrogen, USA) in brain homogenates were measured using Elisa, following the manufacturer's instructions.

2.7. Immunohistochemistry and immunofluorescence

Histological staining was performed as previously described [22,23]. Briefly, the coronal section of the brain was sliced into a 30 μm thickness using a cryosectioning microtome. Five equidistant tissue sections spanning the entire brain were obtained and used for comprehensive histological staining. These sections were separated by approximately 1.3 mm.

Total Aβ plaques were visualized with the 6E10 mouse anti-human Aβ antibody (1:200, BioLegend, USA), while dense Aβ plaques were stained using Congo red (Sigma-Aldrich, USA) staining and thioflavin S

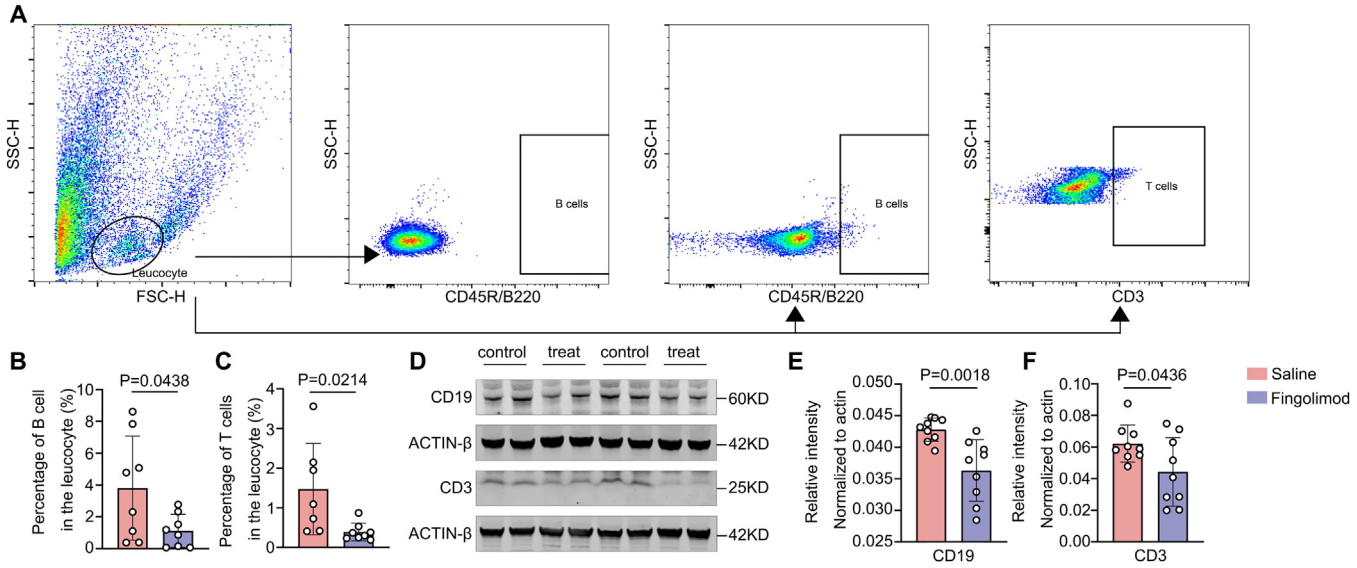

Fig. 2. Fingolimod reduces the infiltration of B lymphocytes in the mouse brain. A. Identification of B and T lymphocytes in the brain after treatment using Flow cytometry. B. Quantification of the percentage of B cells in leucocytes in the brain. C. Quantification of the percentage of T cells in leukocytes in the brain. D. Representative western blot images of CD19 and CD3 in the brain. E and F. Quantitative analyses of CD19 and CD3.

(Sigma, USA). Anti-CD68 antibody (Abcam, UK) was used to observe activated microglia, and anti-GFAP antibody (Abcam, UK) was used to observe activated astrocytes. Tau phosphorylation was detected with anti-pT231 antibody (Signalway, USA), while neuronal cell apoptosis was detected using a NeuN (Abcam, UK) and caspase-3 (Abcam, UK) double-staining approach. Additionally, NeuN and microtubule-associated protein (Map2) (Abcam, UK) double staining was employed to identify neuronal loss and synaptic degeneration. Quantitative analysis was performed by a researcher in a blinded way using Image-Pro Plus 6.0 (National Institutes of Health, USA).

2.8. Brain proteomics

Mouse brain tissue samples were cryogenically pulverized into a fine powder using liquid nitrogen. The resulting tissue powder was lysed and subjected to ultrasonic disruption to ensure thorough cell disintegration and efficient protein extraction. The homogenate was centrifuged to separate the protein-rich supernatant, which was subsequently collected for downstream analyses.

The supernatant, containing brain tissue-derived proteins, underwent enzymatic digestion with trypsin (Thermo Fisher Scientific, USA) to generate a peptide pool. These peptides were desalted to remove contaminants and analyzed using liquid chromatography-tandem mass spectrometry (LC-MS/MS). Specifically, the samples were examined on an Orbitrap Astral mass spectrometer employing data-independent acquisition (DIA) technology. The resulting LC-MS/MS data were processed to construct a sample-specific protein database, which was queried using the DIA-NN software for protein identification and quantification.

Comprehensive quality control procedures were performed at both the peptide and protein levels to ensure data reliability and robustness. Quantitative proteomic analysis was performed to identify differentially abundant proteins. Visualization of these proteins was accomplished through the generation of volcano plots and heatmaps. Differential proteins were subsequently subjected to functional enrichment analyses, including secondary Gene Ontology (GO) classifications and Kyoto Encyclopedia of Genes and Genomes (KEGG) pathway mapping. Gene Set Enrichment Analysis (GSEA) was applied to identify pathways that were different between groups after treatment.

2.9. Statistics

All statistical analyses were conducted using GraphPad Prism (version 8.0.2) or R statistical environment (version 4.0) . Data were assessed for normality with the Shapiro-Wilk test. For all parameters, one-way ANOVA or unpaired t-tests were employed to compare means where appropriate. Multiple time-point comparisons between groups were carried out using two-way ANOVA, with post hoc corrections for multiple comparisons. A P value ≤ 0.05 was considered statistically significant. Results are presented as mean ± SEM.

3. Results

3.1. Fingolimod improves behavioral deficits in APP/PS1 mice

Compared to control mice, fingolimod-treated mice performed better in the Morris water maze test. This was reflected by significant reductions in escape latency in progressive platform learning trials, lower latency of the first entry to the hidden platform, higher distance traveled in the target quadrant, higher numbers of target quadrant entry and annulus crossing in the probe trial (Fig. 1A-H), indicating that the treated group had improved spatial learning ability. In the open filed test, there was no difference in the total distance traveled, frequency of wall exploration, or exploration distance in the central area between the two groups (Fig. 1I–L). In the Y-maze test, the fingolimod-treated group had more time spent in the novel arm than did the control group, reflecting better spatial recognition memory (Fig. 1M). There was no statistical difference in the spontaneous alternation ratio between the two groups (Fig. 1N).

3.2. Fingolimod inhibits the infiltration of lymphocytes into the brain and improves the proteomic network features associated with AD

Fingolimod is known to promote lymphocyte homing in multiple sclerosis, and infiltration of lymphocytes into the brain is associated with increased neuroinflammation. In this study, we confirmed the effects of fingolimod on B and T cell infiltration in the brain through flow cytometry and western blot. As expected, fingolimod treatment resulted in a significant reduction in brain B lymphocytes, as indicated by decreased CD45R-positive staining in flow cytometry and lower CD19 expression

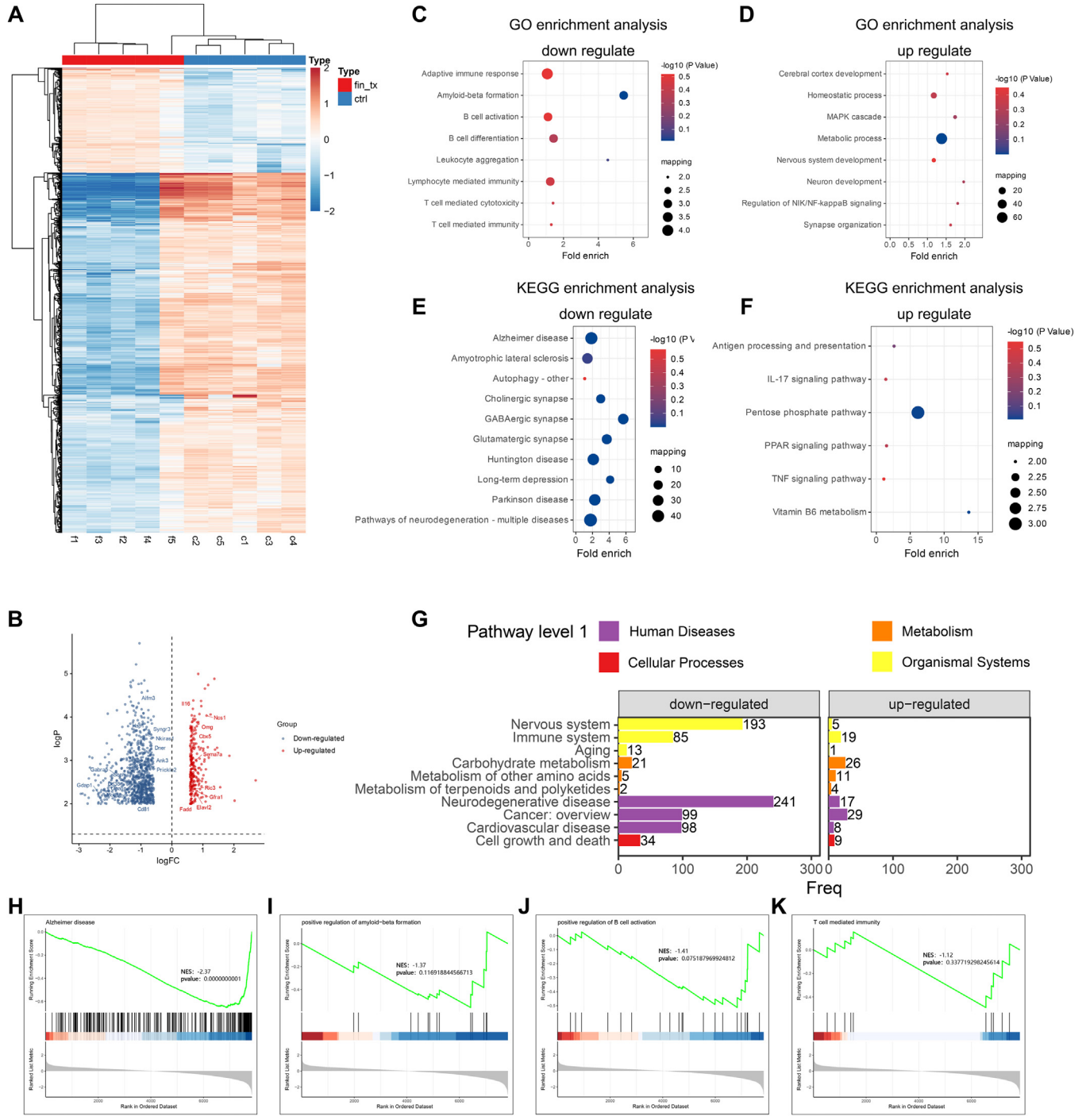

Fig. 3. Proteomic changes after the treatment of fingolimod in the brains of APP/PS1 mice. A. Heat map of protein expression profiles in AD mice after treatment of fingolimod or saline. B. Volcanic plot of gene expression differences in fingolimod-treated AD mice compared to control AD mice. C and D. The downregulation and upregulation of GO enrichment processes in the fingolimod-treated group compared to the control group. E and F. The downregulation and upregulation of KEGG enrichment processes in the fingolimod-treated group compared to the control group. G. Secondary KEGG pathway classification of differentially expressed proteins between the fingolimod- and saline-treated groups. H. The gene set enrichment analysis of Alzheimer's Disease between two groups. I. Gene set enrichment analysis of positive regulation of amyloid β formation. J. Gene set enrichment analysis of positive regulation of B cell activation. K. Gene set enrichment analysis of T cell mediated immunity.

levels in fingolimod-treated mice compared to the control group in western blot analysis (Fig. 2A, B, D, and E). Similarly, the percentage of T lymphocytes in the brain was downregulated following fingolimod treatment, as observed through both flow cytometry and western blot analysis (Fig. 2A, C, D, and F).

Compared to the saline-treated group, a total of 239 upregulated proteins and 821 downregulated proteins were identified in the fingolimod-treated group (Fig. 2A). Notably, surface markers associated with B and T cells, such as CD38 and CD81, were downregulated in the treatment group (Fig. 2B). GO enrichment analysis revealed that biological processes related to B cell activation and differentiation, as well as T cell-mediated immunity, were downregulated in the treatment group. In contrast, processes linked to cerebral cortex development and synapse organization were upregulated (Fig. 2C and D).

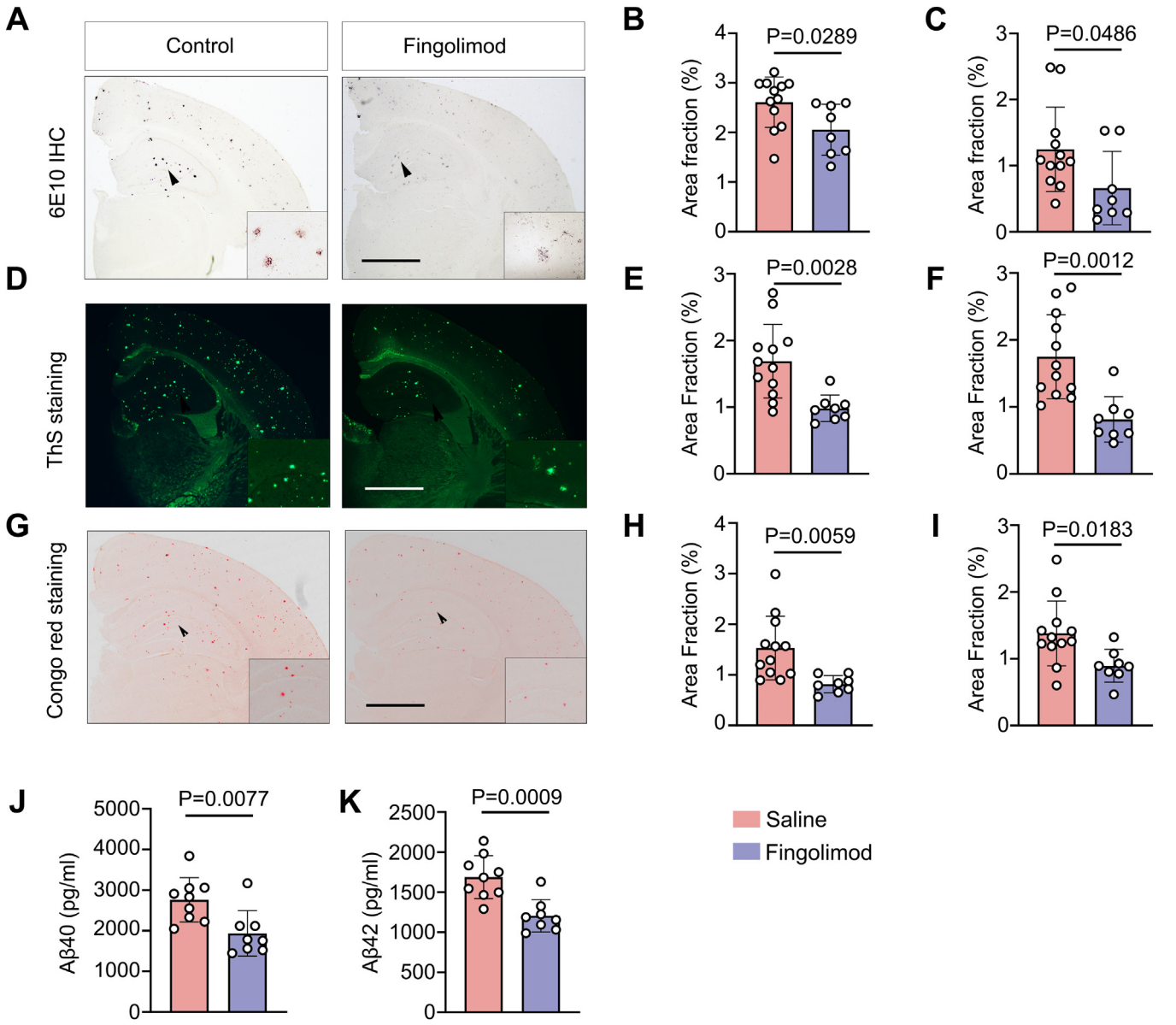

Fig. 4. Fingolimod alleviates brain Aβ deposition in APP/PS1 mice. A. Representative 6E10 immunohistochemical staining images. Scale bar = 500 μm. B and C. Comparison of 6E10 positive area fraction in the neocortex and hippocampus between groups. D. Representative thioflavin S staining images.Scale bar = 500 μm. E and F. Comparison of thioflavin S positive area fraction in the neocortex and hippocampus between groups. G. Representative Congo red staining images. Scale bar = 500 μm. H and I. Comparison of Congo red positive area fraction in the neocortex and hippocampus between groups.

KEGG enrichment analysis further indicated that metabolic pathways associated with AD and other neurodegenerative diseases (Fig. 2E and F). Additionally, secondary GO and KEGG classifications, based on biological processes, cellular components, and molecular functions, revealed a downregulation of pathways associated with neurodegenerative diseases, the immune system, and aging in the treatment group (Fig. 3G). GSEA analysis showed that gene sets related to Alzheimer's disease were downregulated in the treatment group (Fig. 3H–K). Collectively, these findings suggest that fingolimod reduces the infiltration of B and T cells into the brain and downregulates processes associated with AD and neurodegeneration.

3.3. Fingolimod alleviates brain Aβ deposition in APP/PS1 mice

To investigate the effect of fingolimod on Aβ deposition in APP/PS1 mice, we conducted Congo red and THS staining to assess dense amyloid plaques, along with immunohistochemical staining to evaluate total amyloid plaques. The fingolimod-treated group exhibited significantly lower area fractions of 6E10-positive staining in the neocortex and hippocampus (Fig. 4A–C). Similarly, fingolimod-treated group exhibited lower area fractins of THS- and Congo red-positive staining in the neocortex and hippocampus compared to the control group (Fig. 4D–I). Furthermore, the levels of Aβ40 and Aβ42 in brain homogenates were significantly reduced following treatment with fingolimod (Fig. 4J and K).

To assess the effect of fingolimod on APP processing, we measured the expression levels of APP and its processing products in the brain homogenates of APP/PS1 mice. The results indicated that fingolimod did not alter the levels of full-length APP; however, it significantly increased the level of CTF-α while decreasing the level of CTF-β (Fig. 5A–E). The levels of secretases involved in APP processing were further accessed. Fingolimod significantly reduced β-secretase cleavage of APP, as evidenced by decreased expression of BACE1 in the fingolimod-treated group. However, fingolimod did not alter the levels of ADAM10 or PSEN1 (Fig. 5F–I). There were no differences in the levels of proteins

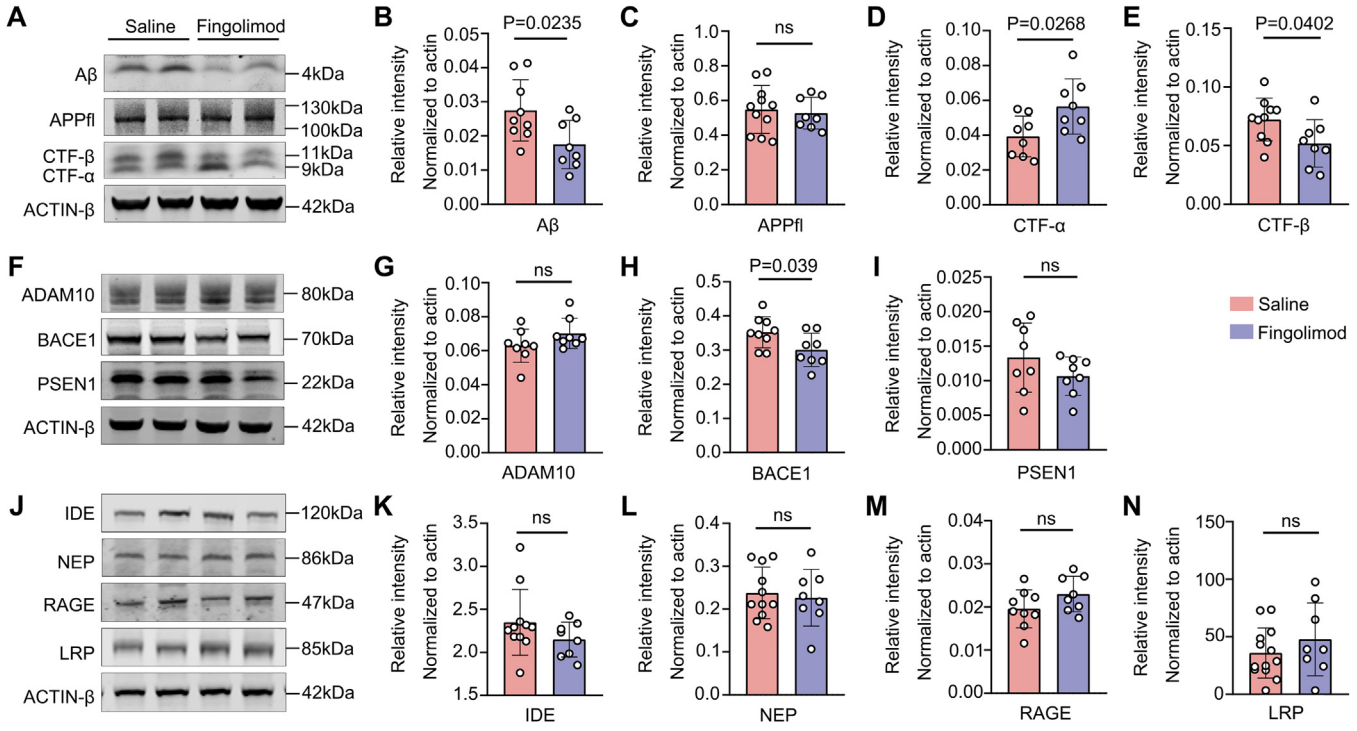

Fig. 5. Fingolimod inhibits amyloidopathogenic pathway in APP/PS1 mice. A. Representative western blot images of full-length APP (APPfl), APP metabolites CTF-α, CTF-β, and Aβ. B-E Quantitative analyses of APPfl, CTF-α, CTF-β, and Aβ. F. Representative western blot images of enzymes involved in APP processing, including ADAM10, BACE1, and PSEN1. G-I. Quantitative analyses of ADAM10, BACE1, and PSEN1. J. Representative western blot images of Aβ-degrading enzymes NEP and IDE, and Aβ transporting molecules LRP and RAGE. K-N. Quantitative analyses of NEP, IDE, LRP, RAGE.

related to Aβ degradation, including NEP and IDE, or proteins involved in Aβ transpotation across the blood-brain barrier, including LRP and RAGE, between the two groups (Fig. 5J–N). These findings suggest that fingolimod reduces Aβ production by shifting APP processing from β-secretase cleavage to α-secretase cleavage.

3.4. Fingolimod attenuates tau hyperphosphorylation in the brains of APP/PS1 mice

We next determined the effects of fingolimod on Tau hyperphosphorylation in the brain. Western blot was used to measure the levels of Tau phosphorylation at at multiple sites. The levels of total Tau (Tau5), Tau hyperphosphorylation at Ser404 (PS404), Thr231 (PT231), Ser199 (PS199), and Thr181 (PT181) were reduced following fingolimod treatment (Fig. 6A–H). Consistently, PT231 staining revealed a significant reduction in both the PT231-positive area fractions and the average size of positive staining in the hippocampus and neocortex of fingolimod-treated mice (Fig. 6I–K). These findings indicate that fingolimod treatment rescued Tau hyperphosphorylation in APP/PS1 mice.

3.5. Fingolimod alleviates neuroinflammation and improves the integrity of neuronal networks in the brains of APP/PS1 mice

We explored the effects of fingolimod on brain neuroinflammation and the integrity of neuornal network in APP/PS1 mice. We found that the area fraction of both GFAP (Fig. 7A–C) and CD68 positive staining (Fig. 7D-F) in the neocortex and hippocampus were reduced following fingolimod treatment, suggesting that fingolimod reduce the level of gliosis in the brain. In addition, we measured the levels of TNF-α and IL-1β in brain homogenates and found that TNF-α levels were reduced, while IL-1β levels remained unchanged following treatment with fingolimod (Fig. 7G and H).

Compared to the control group, the area fraction of Map2-positive staining in the hippocampal CA1 region was increased in mice treated with fingolimod (Fig. 8A and B). Additionally, the area fraction of activated caspase-3 was reduced, while the area fraction of NeuN-positive staining was increased in the hippocampal CA3 region (Fig. 8C–E). We also found that the levels of synapse-related proteins PSD95, SNAP25, and VAMP1 in the fingolimod-treated group were higher than those in the control group (Fig. 8F–J). These findings indicate that fingolimod alleviates neuroinflammation and neurodegeneration, while also improving neuronal network integrity in APP/PS1 mice,

4. Discussion

In this study, we examined the effect of fingolimod, a S1P receptor antagonist, on behavioral deficits and AD-type pathologies in the APP/PS1 mouse model. The results demonstrated that treatment with fingolimod improves memory deficits, alleviates amyloidosis, Tau hyperphosphorylation, and neuroinflammation, and restores the integrity of neuonal network in the brain.

Systemic inflammation is linked to the development of AD, leading to the formulation of the inflammation hypothesis for AD [24,25]. The immune system plays a crucial role in regulating inflammation, with lymphocytes serving as key components in this process. The phenotypes of B [26] and T lymphocytes [27] in AD patients differ significantly from those in healthy adults. The infiltration of lymphocytes into the brain promote the development of AD [28,29]. They contribute to the pathogenesis of AD through various mechanisms, including the promotion of neuroinflammation and autoimmune attack to the CNS [28].

The role of B lymphocyte in the pathogenesis of AD has gained substantial evidence in recent years [11]. Our group had identified several autoantibodies that are pathogenic in AD patients [6–8,22]. Besides, the gene expression profile of B lymphocytes is reported to be altered during the development of the disease [26]. A recent study has indicated that depletion of B lymphocyte aid in alleviation of AD-type pathologies [12], suggesting that CD19- or CD20-targeted therapies may hold promise for the treatment of AD. The function of T

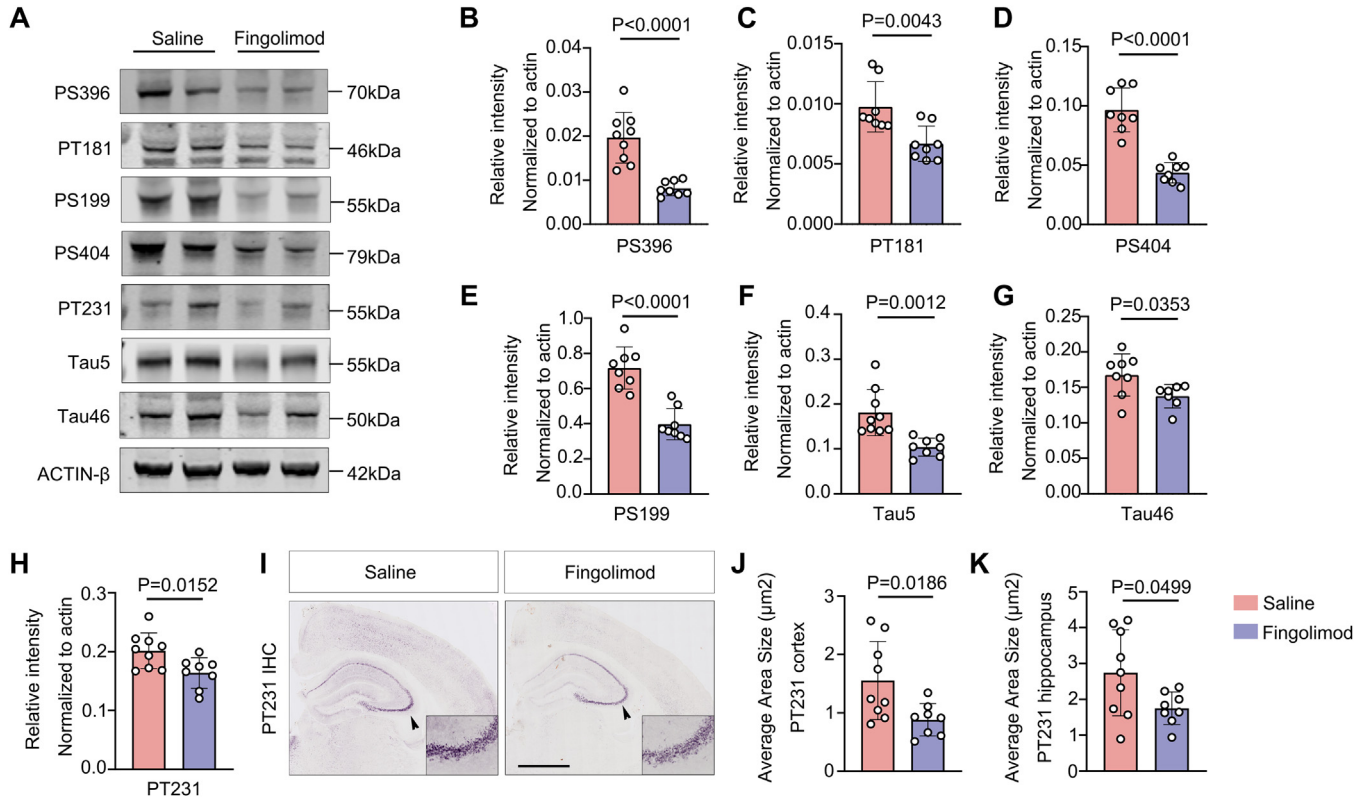

Fig. 6. Fingolimod attenuates tau hyperphosphorylation in the brains of APP/PS1 mice. A. Representative western blot images of total Tau (Tau5 and Tau46) and phosphorylated Tau (PS396, PT181, PS199, PS404, and PT231) protein at multiple sites. B-H Quantitative analyses of total Tau and phosphorylated Tau protein at multiple sites. I. Representative PT231 immunohistochemical staining images. Scale bar = 500 μm. J-K. Comparison of area fraction and plaque size of PT231 positive staining in the neocortex and hippocampus between groups.

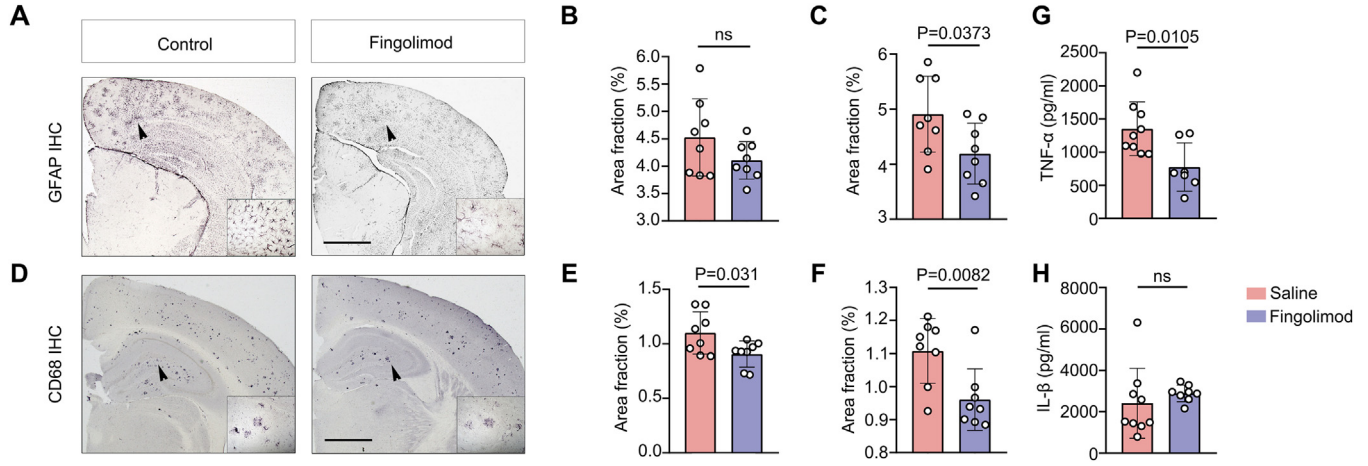

Fig. 7. Fingolimod alleviates neuroinflammation in the brains of APP/PS1 mice. A. Representative GFAP immunohistochemical staining images. Scale bar = 500 μm. B and C. Comparison of GFAP positive area fraction in the neocortex and hippocampus between groups. D. Representative CD68 immunohistochemical staining images. Scale bar = 500 μm. E and F. Comparison of CD68 positive area fraction in the neocortex and hippocampus between groups.

lymphocytes in AD has also been investigated in recent years. Antigen-specific age-related memory CD8 T cells are found to induce and track AD-like neurodegeneration [30]. Infiltration of T lymphoctes into the brain exacerbates AD-type pathologies [29] while restraining CD4+ T cell-mediated neuroinflammation could improve the pathogenesis of AD [31].

Fingolimod binds to S1P receptors, preventing lymphocytes from exiting lymph nodes and entering systemic circulation. Moreover, it can partially modulate the restriction of blood B and T lymphocytes from crossing the blood-brain barrier and entering the brain [32,33]. In this study, we observed a significant reduction in brain B and T lymphocytes following fingolimod treatment. Based on this, we proposed that fingolimod may have disease-modifying effects in the treatment of AD. Indeed, fingolimod improves learning abilities and working memories of APP/PS1 mice. It alleviates multiple AD-related pathologies, including Aβ deposition, Tau hyperphosphorylation, neuroinflammation (GFAP and CD68), and neuronal and synaptic loss. Furthermore, the proteomic analysis indicated that multiple pathways associated with AD were downregulated following fingolimod treatment. Although previous studies have demonstrated the potential protective effects of fingolimod

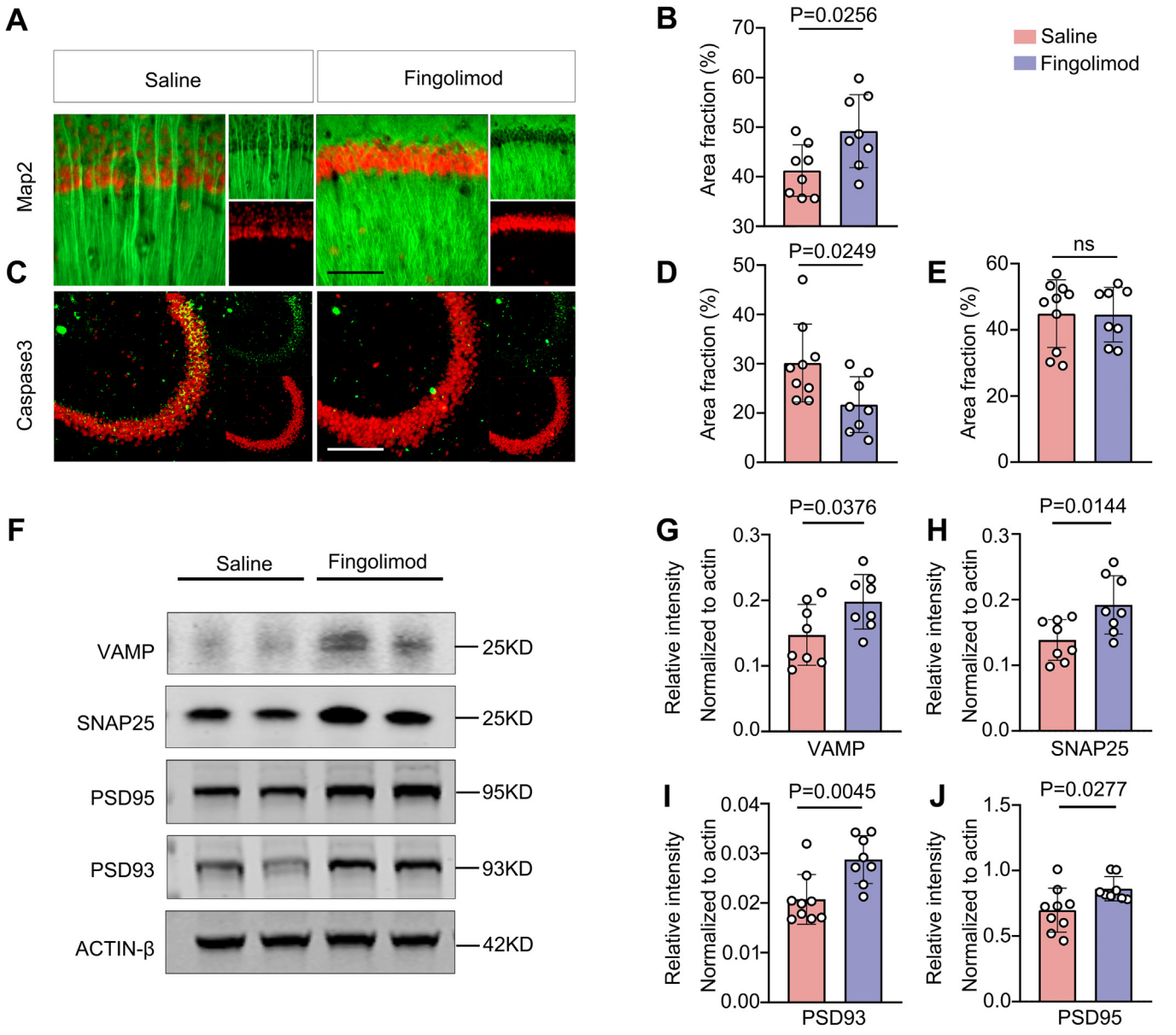

Fig. 8. Fingolimod improves the integrity of neuronal networks in the brains of APP/PS1 mice. A. Representative images of NeuN and Map2 immunofluorescence staining in the CA1 region of the hippocampus. Scale bar = 50 μm. B. Comparison of Map2 positive area fraction in the CA1 region of hippocampus between groups. C. Representative images of NeuN and caspase-3 immunofluorescence staining in the CA3 region of the hippocampus. D. Comparison of caspase-3 positive area fraction in the CA3 region of hippocampus between groups. Scale bar = 100 μm. E. Comparison of NeuN positive area fraction in the CA1 region of hippocampus between groups. F. Representative western blot images of synapes-associated proteins (VAMP1, SNAP25, PSD95, and PSD93). G-J. Quantitative analyses of VAMP1, SNAP25, PSD95, and PSD93.

on AD, our research provides a detailed landscape of its protective effects on AD from multiple perspectives.

The potential mechanisms underlying the effects of fingolimod in the treatment of AD may involve additional pathways. As previously reported, fingolimod inhibit neuroinflammation that is detrimental in AD by promoting Aβ production via increasing the activities of BACE1 [34] and γ-secretase [35]. In this study, we found that the expression of BACE1 was decreased following fingolimod treatment, thus suggesting fingolimod might exhibit protective effects by inhibiting Aβ production. Besides, previous studies also demonstrate that fingolimod protect the glial cells from overactivation, thus might enchance their phagocytic functions [36]. Our findings that CD68 and GFAP positive area are decreased after treatment, which is consistent with previous studies. Furthermore, fingolimod can activate the neurotrophic pathways such as promoting BDNF expression [37].

Repurposing clinically approved drugs for AD is an effective strategy to expedite the implementation of available treatments into clinical practice while minimizing the risk of adverse effects often observed in clinical trials of novel drug candidates [38]. The present findings, along with previous studies, suggest that fingolimod can improve key pathological pathways in AD, positioning it as a promising clinical intervention. This study also suggests that the immune system may play a critical role in the pathogenesis of AD. Emerging evidence highlights the divergent roles of lymphocyte subsets in AD. For instance, CD8+ T cells have been reported to limit Aβ deposition [39], while other studies suggest they exacerbate pathology [14]. Given these conflicting findings, the broad suppression of lymphocyte infiltration proposed in this study may lack nuance. A more targeted analysis of specific lymphocyte subtypes (e.g., regulatory vs. cytotoxic populations) would strengthen the mechanistic interpretation and align the conclusions with recent advances in

the field. Additionally, it lacks clinical evidence, highlighting the need for clinical trials to assess the effects of fingolimod on AD pathologies and clinical outcomes.

Declaration of generative AI and AI-assisted technologies in the writing process

I have not used any AI in the writing of the manuscript.

Declaration of competing interest

The authors declare the following financial interests/personal relationships which may be considered as potential competing interests:

Yu-Hui Liu reports financial support was provided by National Natural Science Foundation of China. If there are other authors, they declare that they have no known competing financial interests or personal relationships that could have appeared to influence the work reported in this paper.

CRediT authorship contribution statement

Meng-Ting Wang: Investigation. **Zi-Cheng Hu:** Formal analysis. **Yang Xiang:** Formal analysis. **Xiao-Qin Zeng:** Investigation. **Zhang-Cheng Fei:** Visualization. **Jia Chen:** Investigation. **Xin-Peng Li:** Investigation. **Yu-Peng Zhu:** Visualization. **Jun Wang:** Writing – review & editing. **Yan-Jiang Wang:** Writing – review & editing. **Zhi-Qiang Xu:** Writing – original draft, Conceptualization. **Yu-Hui Liu:** Writing – original draft, Conceptualization.

Data availability

The raw data supporting the findings of this study are available upon reasonable request to the corresponding authors.

Acknowledgement

This study was supported by the National Natural Science Foundation of China (82222023 and 82471461 to Y.H.L.), the National-Level Reserve Talent Program of the Chongqing Health Commission (HBRC202402 to Y.H.L.), the Natural Science Foundation of Chongqing (no CSTB2022NSCQ-LZX0042 to LYH), Project of Sichuan Department of Science and Technology (no 2023YFS0267 and 2022NSFSC1374 to Y.X.), Project of Sichuan Provincial Health Commission (no 21PJ086 to Y.X.), and the Key Clinical Specialty of Neurology of PLA to Daping Hospital.

References

[1] Jia L, Quan M, Fu Y, Zhao T, Li Y, Wei C, et al. Dementia in China: epidemiology, clinical management, and research advances. Lancet Neurol 2020;19:81–92. doi:10.1016/S1474-4422(19)30290-X.
[2] Sanabria-Castro A, Alvarado-Echeverría I, Monge-Bonilla C. Molecular pathogenesis of Alzheimer's disease: an update. Ann Neurosci 2017;24:46–54. doi:10.1159/000464422.
[3] Lane CA, Hardy J, Schott JM. Alzheimer's disease. Eur J Neurol 2018;25:59–70. doi:10.1111/ene.13439.
[4] DeTure MA, Dickson DW. The neuropathological diagnosis of Alzheimer's disease. Mol Neurodegener 2019;14:32. doi:10.1186/s13024-019-0333-5.
[5] Goldwaser EL, Acharya NK, Wu H, Godsey GA, Sarkar A, DeMarshall CA, et al. Evidence that brain-reactive autoantibodies contribute to chronic neuronal internalization of exogenous amyloid-β1-42 and key cell surface proteins during Alzheimer's disease pathogenesis. JAD 2020;74:345–61. doi:10.3233/JAD-190962.
[6] Liu Y-H, Wang J, Li Q-X, Fowler CJ, Zeng F, Deng J, et al. Association of naturally occurring antibodies to β-amyloid with cognitive decline and cerebral amyloidosis in Alzheimer's disease. Sci Adv 2021;7 eabb0457. doi:10.1126/sciadv.abb0457.
[7] Wang Y-R, Wang M-T, Zeng X-Q, Liu Y-H, Wang Y-J. Associations of naturally occurring antibodies to presenilin-1 with brain amyloid-β load and cognitive impairment in Alzheimer's disease. J Alzheimers Dis 2022;90:1493–500. doi:10.3233/JAD-220775.
[8] Liu Y-H, Bu X-L, Liang C-R, Wang Y-R, Zhang T, Jiao S-S, et al. An N-terminal antibody promotes the transformation of amyloid fibrils into oligomers and enhances the neurotoxicity of amyloid-beta: the dust-raising effect. J Neuroinflamm 2015;12:153. doi:10.1186/s12974-015-0379-4.
[9] Liu Y-H, Zeng F, Wang Y-R, Zhou H-D, Giunta B, Tan J, et al. Immunity and Alzheimer's disease: immunological perspectives on the development of novel therapies. Drug Discov Today 2013;18:1212–20. doi:10.1016/j.drudis.2013.07.020.
[10] Ma Y-Z, Cao J-X, Zhang Y-S, Su X-M, Jing Y-H, Cells Gao L-PT. Trafficking into the brain in aging and Alzheimer's disease. J Neuroimmun Pharmacol 2024;19:47. doi:10.1007/s11481-024-10147-5.
[11] Park J-C, Noh J, Jang S, Kim KH, Choi H, Lee D, et al. Association of B cell profile and receptor repertoire with the progression of Alzheimer's disease. Cell Rep 2022;40:111391. doi:10.1016/j.celrep.2022.111391.
[12] Kim K, Wang X, Ragonnaud E, Bodogai M, Illouz T, DeLuca M, et al. Therapeutic B-cell depletion reverses progression of Alzheimer's disease. Nat Commun 2021;12:2185. doi:10.1038/s41467-021-22479-4.
[13] Kedia S, Ji H, Feng R, Androvic P, Spieth L, Liu L, et al. T cell-mediated microglial activation triggers myelin pathology in a mouse model of amyloidosis. Nat Neurosci 2024;27:1468–74. doi:10.1038/s41593-024-01682-8.
[14] Jorfi M, Park J, Hall CK, Lin C-CJ, Chen M, von Maydell D, et al. Infiltrating CD8+ T cells exacerbate Alzheimer's disease pathology in a 3D human neuroimmune axis model. Nat Neurosci 2023;26:1489–504. doi:10.1038/s41593-023-01415-3.
[15] Liu Y-H, Giunta B, Zhou H-D, Tan J, Wang Y-J. Immunotherapy for Alzheimer disease—the challenge of adverse effects. Nat Rev Neurol 2012;8:465–9. doi:10.1038/nrneurol.2012.118.
[16] Brinkmann V. FTY720 (fingolimod) in multiple sclerosis: therapeutic effects in the immune and the central nervous system. Br J Pharmacol 2009;158:1173–82. doi:10.1111/j.1476-5381.2009.00451.x.
[17] Nishihara H, Shimizu F, Sano Y, Takeshita Y, Maeda T, Abe M, et al. Fingolimod prevents blood-brain barrier disruption induced by the sera from patients with multiple sclerosis. PLoS One 2015;10:e0121488. doi:10.1371/journal.pone.0121488.
[18] van Doorn R, Nijland PG, Dekker N, Witte ME, Lopes-Pinheiro MA, van het Hof B, et al. Fingolimod attenuates ceramide-induced blood-brain barrier dysfunction in multiple sclerosis by targeting reactive astrocytes. Acta Neuropathol 2012;124:397–410. doi:10.1007/s00401-012-1014-4.
[19] Janus C., Chishti M.A., Westaway D. Transgenic mouse models of Alzheimer's disease. Biochimica et Biophysica Acta n.d.
[20] Carreras I, Aytan N, Choi J-K, Tognoni CM, Kowall NW, Jenkins BG, et al. Dual dose-dependent effects of fingolimod in a mouse model of Alzheimer's disease. Sci Rep 2019;9:10972. doi:10.1038/s41598-019-47287-1.
[21] Aytan N, Choi J-K, Carreras I, Brinkmann V, Kowall NW, Jenkins BG, et al. Fingolimod modulates multiple neuroinflammatory markers in a mouse model of Alzheimer's disease. Sci Rep 2016;6:24939. doi:10.1038/srep24939.
[22] Jian J-M, Fan D-Y, Tian D-Y, Cheng Y, Sun P-Y, Tan C-R, et al. Naturally-occurring antibodies against bim are decreased in Alzheimer's disease and attenuate AD-type pathology in a mouse model. Neurosci Bull 2022;38:1025–40. doi:10.1007/s12264-022-00869-y.
[23] Yu Z-Y, Yi X, Wang Y-R, Zeng G-H, Tan C-R, Cheng Y, et al. Inhibiting α1-adrenergic receptor signaling pathway ameliorates AD-type pathologies and behavioral deficits in APPswe/PS1 mouse model. J Neurochem 2022;161:293–307. doi:10.1111/jnc.15603.
[24] Leng F, Edison P. Neuroinflammation and microglial activation in Alzheimer disease: where do we go from here? Nat Rev Neurol 2021;17:157–72. doi:10.1038/s41582-020-00435-y.
[25] Heppner FL, Ransohoff RM, Becher B. Immune attack: the role of inflammation in Alzheimer disease. Nat Rev Neurosci 2015;16:358–72. doi:10.1038/nrn3880.
[26] Xiong L-L, Xue L-L, Du R-L, Niu R-Z, Chen L, Chen J, et al. Single-cell RNA sequencing reveals B cell-related molecular biomarkers for Alzheimer's disease. Exp Mol Med 2021;53:1888–901. doi:10.1038/s12276-021-00714-8.
[27] Leffell MS, Lumsden L, Steiger WA. An analysis of T lymphocyte subpopulations in patients with Alzheimer's disease. J Am Geriatr Soc 1985;33:4–8. doi:10.1111/j.1532-5415.1985.tb02851.x.
[28] Zhang H, Cao F, Zhou Y, Wu B, Li C. Peripheral immune cells contribute to the pathogenesis of Alzheimer's disease. Mol Neurobiol 2024. doi:10.1007/s12035-024-04266-6.
[29] Zeng J, Liao Z, Yang H, Wang Q, Wu Z, Hua F, et al. T cell infiltration mediates neurodegeneration and cognitive decline in Alzheimer's disease. Neurobiol Dis 2024;193:106461. doi:10.1016/j.nbd.2024.106461.
[30] Panwar A, Rentsendorj A, Jhun M, Cohen RM, Cordner R, Gull N, et al. Antigen-specific age-related memory CD8 T cells induce and track Alzheimer's-like neurodegeneration. Proc Natl Acad Sci U S A 2024;121:e2401420121. doi:10.1073/pnas.2401420121.
[31] Kuang Y, Zhu M, Gu H, Tao Y, Huang H, Chen L. Alkaloids in Uncaria rhynchophylla improves AD pathology by restraining CD4+ T cell-mediated neuroinflammation via inhibition of glycolysis in APP/PS1 mice. J Ethnopharmacol 2024;331:118273. doi:10.1016/j.jep.2024.118273.
[32] Bravo GÁ, Cedeño RR, Casadevall MP. Ramió-Torrentà L. Sphingosine-1-Phosphate (S1P) and S1P Signaling Pathway Modulators, from Current Insights to Future Perspectives. Cells 2022;11:2058. doi:10.3390/cells11132058.
[33] Chiba K. FTY720, a new class of immunomodulator, inhibits lymphocyte egress from secondary lymphoid tissues and thymus by agonistic activity at sphingosine 1-phosphate receptors; 2005.
[34] Deardorff WJ, Grossberg GT. Targeting neuroinflammation in Alzheimer's disease: evidence for NSAIDs and novel therapeutics. Expert Rev Neurother 2017;17:17–32. doi:10.1080/14737175.2016.1200972.
[35] Hur J-Y, Frost GR, Wu X, Crump C, Pan SJ, Wong E, et al. The innate immunity protein IFITM3 modulates γ-secretase in Alzheimer's disease. Nature 2020;586:735–40. doi:10.1038/s41586-020-2681-2.
[36] Carreras I, Jung Y, Lopez-Benitez J, Tognoni CM, Dedeoglu A. Fingolimod mitigates memory loss in a mouse model of Gulf War Illness amid decreasing the activa-

tion of microglia, protein kinase R, and NFκB. Neurotoxicology 2023;96:197–206. doi:10.1016/j.neuro.2023.05.006.
[37] Yu X, Qi X, Wei L, Zhao L, Deng W, Guo W, et al. Fingolimod ameliorates schizophrenia-like cognitive impairments induced by phencyclidine in male rats. Br J Pharmacol 2023;180:161–73. doi:10.1111/bph.15954.
[38] Leßmann V, Kartalou G-I, Endres T, Pawlitzki M, Gottmann K. Repurposing drugs against Alzheimer's disease: can the anti-multiple sclerosis drug fingolimod (FTY720) effectively tackle inflammation processes in AD? J Neural Transm (Vienna) 2023;130:1003–12. doi:10.1007/s00702-023-02618-5.
[39] Su W, Saravia J, Risch I, Rankin S, Guy C, Chapman NM, et al. CXCR6 orchestrates brain CD8+ T cell residency and limits mouse Alzheimer's disease pathology. Nat Immunol 2023;24:1735–47. doi:10.1038/s41590-023-01604-z.